Modeling and optimization of the delivery fluctuation of gear pumps

Efstratios Tsolakis[1]*, *Antonios* Tzanopoulos[1], *Georgios* Vasileiou[1], *Nikolaos* Rogkas[1], *Vasilios* Spitas[1], and *Pavlos* Zalimidis[2]

[1]National Technical University of Athens, School of Mechanical Engineering, Laboratory of Machine Design, 9 Iroon Polytechneiou, 15780 Athens, Greece
[2]School of Pedagogical and Technological Education, Department of Mechanical Engineering Educators, Iraklio Attikis, 14121 Athens, Greece

Abstract. Presented work aims to minimize the delivery fluctuation of a gear pump through geometrical optimisation of the tooth flank. Therefore, instead of examining various configurations, which would reduce the flow ripple ad hoc , the current study suggests the dependence the delivery fluctuation to the tooth flank profile. Taking into account the secondary derivative of the tooth profile, the optimisation process is able to also affect the secondary delivery fluctuation, which is connected to the compression of the fluid over the meshing cycle. Bezier-Bernstein polynomial curves were used to model the tooth flank in order to satisfy the objective function. A dependency between the total length of the path of contact curve and the flow ripple was found. It is stated in this work that for every design point on a closed path of gear set, there is a threshold on the contact length, over which the resulted flow ripple starts to deviate from the optimum value. That conclusion was used to further enhance the optimisation algorithm. The presented optimum gear profile design was evaluated through a comparative study between every design point and the corresponding solution of the existing state of the art in terms of delivery fluctuation.

1 Introduction

External gear pumps are widely used in high pressure hydraulic applications. The main reason are their simple design and their ability to carry medium to high pressures (up to 350 bar) at low to medium delivery rates (oil flow). However, as positive displacement systems, their main drawback is that they are associated with delivery fluctuation, which is responsible to pressure fluctuation and therefore noise and vibration in the upstream system.

For years this issue has been tackled using various designs that include among others, tooth forms different than involute ones [1, 2, 6], addendum modifications (shifted teeth) [1, 4], non-conjugate gears [3, 7] and helical gear tooth design (or herringbone) [2]. Also, some non-geometrical solutions have been proposed to address the problem on a systems level including use of oil accumulators and internal/ external controlled leakages [5], however the inherent complexity, cost and reduced adaptability over a wide range of speeds, flow-rates and pressures have rendered the use of the above solutions very limited in practice.

Presented work aims to minimize this delivery pulsation through geometrical optimisation of the tooth flank, therefore to tackle the inherent nature of the phenomenon which is the non-constant surface of the teeth engaged in the meshing cycle. Therefore, instead of examining various configurations, which would reduce the flow ripple ad hoc, the current study suggests the dependence of the delivery fluctuation on the tooth flank profile.

2 Flow ripple in symmetrical tooth profiles

2.1 General

When conjugate gear have close path of contact, they have the advantage that they do not carry return flow from pressure to return chamber since their tooth profile remains in contact throughout the whole meshing cycle. To the contrary, in cases like involute gears, the path of contact is a line, or an open curve in general, thus a backflow is constantly present. Additionally, during the engagement of open path of contact gears, the contact ratio is higher than 1, thus a fluid volume is always trapped between the engaged gears. Since this volume is not constant during the engagement, it compression and expansion results in non-constant reaction forces and moments during the meshing cycle which also contributes to the decrease of pump's overall efficiency.

* Corresponding author: etsolakis@central.ntua.gr

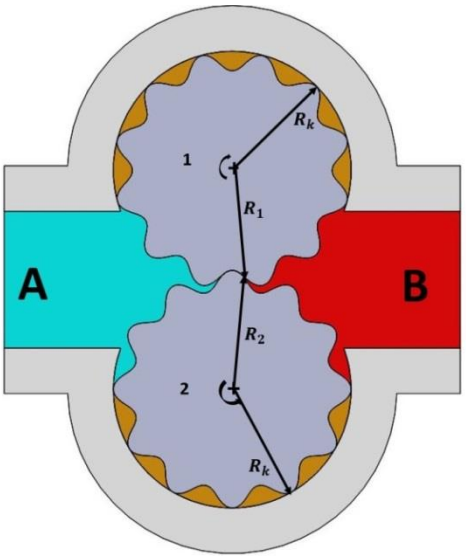

Fig. 1. Characteristic properties of closed path of contact gear pump.

As a result, in gear pumps of closed path of contact, the backflow is minimized to the extent that it is only depended on the leakage occurring between tooth tip and the housing. From fig. 1 it is derived that A describes suction volume, B describes pressure volume and R_k describes the tooth tip of the meshing gears. By the infinitesimal pump rotation on $d\theta$, the flow delivery is depended on two terms. The first term describes the increase of fluid volume on chamber B by:

$$dV_{in} = 2\left(R_K{}^2 \frac{d\theta}{2}\right) = R_K{}^2 d\theta \quad (1)$$

The second term describes the decrease of fluid volume on chamber B by:

$$dV_{out} = \left[R_1{}^2(\theta) + R_2{}^2(\theta)\right]\frac{d\theta}{2} \quad (2)$$

By $R_1(\theta)$ and $R_2(\theta)$ we describe the radiuses on the point of contact that correspond to each gear. Defining the pitch circle radius R_0, we obtain:

$$R_1{}^2(\theta) = \left(Y\frac{dY}{dX}\right)^2 + (Y + R_o)^2 \quad (3)$$

$$R_2{}^2(\theta) = \left(Y\frac{dY}{dX}\right)^2 + (Y - R_o)^2 \quad (4)$$

Coordinates X,Y along with $\frac{dY}{dX}$, refer to the profile point of the rack that generates the corresponding points of the meshing profiles that merge at this specific point of the path of contact. Thus, the flow delivery can be written as:

$$\frac{dV}{d\theta} = \frac{dV_{in}}{d\theta} - \frac{dV_{out}}{d\theta} = R_K{}^2 - \frac{R_1{}^2(\theta) + R_2{}^2(\theta)}{2} \quad (5)$$

and therefore as:

$$\frac{dV}{d\theta} = R_K{}^2 - R_o{}^2 - \left[\left(Y\frac{dY}{dX}\right)^2 + Y^2\right] = R_K{}^2 - R_o{}^2 - \beta^2 \quad (6)$$

Where β is the distance between the point of contact and the pitch circle center:

$$\beta^2 = \left(Y\frac{dY}{dX}\right)^2 + Y^2 \quad (7)$$

Deviation of this length is finally to be accounted for the preliminary delivery fluctuation of the gear pump. Maximum flow delivery appears when β equals to 0, where the point of contact lays on the pitch circle and the corresponding value is:

$$\frac{dV}{d\theta_{max}} = R_K{}^2 - R_o{}^2 \quad (8)$$

The minimum delivery flow appears when β becomes maximum, thus:

$$\frac{dV}{d\theta_{min}} = R_K{}^2 - R_o{}^2 - \beta_{max}{}^2 \quad (9)$$

For the purpose of the study, only symmetrical tooth profiles are taken into account. In such cases tooth height equal with root depth, thus:

$$a = b \quad (10)$$

As a result:

$$\beta_{max} = R_K - R_o = \alpha \quad (11)$$

And the minimum flow delivery is obtained:

$$\frac{dV}{d\theta_{min}} = R_K{}^2 - R_o{}^2 - (R_K - R_o)^2 = 2aR_o \quad (12)$$

The following fig. 2 depicts a representative chart for delivery fluctuation in symmetrical tooth profile gear pumps.

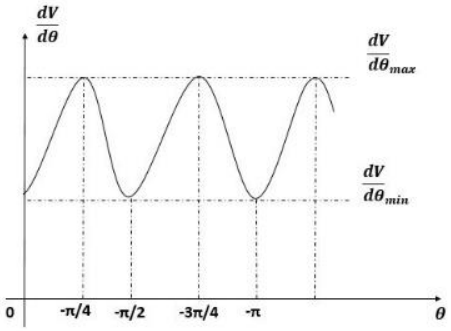

Fig. 2. Typical flow ripple graph for a closed path of contact gear pump.

2.2 Symmetrical tooth profiles

For symmetrical tooth profiles, it can be said that two segments, AB and BC, characterize them. A starts at the intersection with the root circle, B is the intersection point with the pitch circle and C is the intersection with tooth tip circle. That segment BC is uniquely defined by segment AB and vice versa. This generation is straightforward assumption using the Theory of Gearing. In the algorithms that were developed, segment BC was generated and segmented AB was generated based on the conditions that defined the gear meshing. As it was noted, restriction on symmetry, by definition lead to the relation $a=b$.

As is stated, A is the intersection of tooth profile with the root circle, C is its intersection with the tip circle and B is its intersection with pitch circle. The angles of AB and AC with the gear center, are equal and their value is $\frac{\pi}{Z}$ (half of the "half tooth angle"). This is true irrespectively of the type of curves that are used to generate the gears (sinusoidal, polynomial etc.) as long as they can describe close path of contact symmetrical gears. The coordinates for points C and B are given as follows:

$$(C) = (0, R_k) \quad (13)$$

$$x_B = -R_o \sin\left(\frac{\pi}{2Z}\right) \quad (14)$$

$$y_B = R_o \cos\left(\frac{\pi}{2Z}\right) \quad (15)$$

It can easily be observed that given the above characteristics for the profile, the only free parameters to describe the gear envelope are Z and R_k. Further information for symmetrical profiles can be found on [10].

3 Bezier Curve Tooth Profiles

3.1 Bezier Polynomials

Bezier-Berstein curves is a simple way of approximating a geometrical shape using multiple control-points [9]. One key property of these curves is that they start from the first control point and the end in the last. These two control point also define the slope of the curve at its beginning and end. Assuming *N+1* control points and $\vec{r_i} = (x_i, y_i)$ being one of these, the Bezier curve is given as follows:

$$x(t) = \sum_{i=0}^{N} x_i C_i(t) \quad (16)$$

and

$$y(t) = \sum_{i=0}^{N} y_i C_i(t) \quad (17)$$

where:

$$\begin{bmatrix} C_o(t) \\ C_1(t) \\ \vdots \\ C_N(t) \end{bmatrix} = \begin{bmatrix} m_{0,0} & m_{0,1} & \dots & m_{0,N} \\ m_{1,0} & m_{1,1} & \dots & m_{1,N} \\ \vdots & \vdots & \vdots & \vdots \\ m_{N,0} & m_{N,1} & \dots & m_{N,N} \end{bmatrix} \begin{bmatrix} t^0 \\ t^1 \\ \vdots \\ t^N \end{bmatrix} \quad (18)$$

and:

$$m_{i,j} = (-1)^{j-i} \binom{N}{j} \binom{j}{i} \quad (19)$$

Parameter *t* takes its values in the interval [0,1], thus for *t=0* we deduct the first Bezier point and for *t=1* the last. For the scope of the study 4 control points where used and the matrix of equation 18 is:

$$\begin{bmatrix} C_o(t) \\ C_1(t) \\ C_2(t) \\ C_3(t) \end{bmatrix} = \begin{bmatrix} 1 & -3 & 3 & -1 \\ 0 & 3 & -6 & 3 \\ 0 & 0 & 3 & -3 \\ 0 & 0 & 0 & 1 \end{bmatrix} \begin{bmatrix} t^0 \\ t^1 \\ t^2 \\ t^3 \end{bmatrix} \quad (20)$$

Therefore, using the equations 16 and 17, the parametric relations that describe the Bezier curve are:

$$x(t) = (1 - 3t + 3t^2 - t^3)x_0 + (3t - 6t^2 + 3t^3)x_1 + (3t^2 - 3t^3)x_2 + (t^3)x_3 \quad (21)$$

and:

$$y(t) = (1 - 3t + 3t^2 - t^3)y_0 + (3t - 6t^2 + 3t^3)y_1 + (3t^2 - 3t^3)y_2 + (t^3)y_3 \quad (22)$$

In order to define the normal vectors of the Bezier curves, the first derivative of these equations has to be obtained:

$$\frac{dx}{dt} = (-3 + 6t - 3t^2)x_0 + (3 - 12t + 9t^2)x_1 + (6t - 9t^2)x_2 + (3t^2)x_3 \quad (23)$$

and:

$$\frac{dy}{dt} = (-3 + 6t - 3t^2)y_0 + (3 - 12t + 9t^2)y_1 + (6t - 9t^2)y_2 + (3t^2)y_3 \quad (24)$$

Since the curve generates segment BC, it is evident that the first control point P_0 coincides with profile point *B* and the last control point P_3 coincides with profile point C. Thus:

$$P_0 = \left(-R_o \sin\left(\frac{\pi}{2Z}\right), R_o \cos\left(\frac{\pi}{2Z}\right)\right) \quad (25)$$

and:

$$P_3 = (0, R_K) \quad (26)$$

P_2 defines the slope for the last point. Furthermore, in order to have close path of contact, the final point should be of zero slope. As a result, P_2 is by default laying on line that starts from P_3 and is parallel to *x*-axis. Additionally the limits for the P_2 value, define the x-components of P_0 and P_3. Substituting the resulting interval into equal segments, we obtain a range for possible values for P_2. By dividing the vertical lines that define the x-components of possible P_2 values into equal segments the limits of which are the y-components of P_0 and P_3, we define and area of possible values for P_1 for tooth number equal to 6. This possible value number for P_1 and P_2 gives the ability to create significant number for Bezier curves which can be increased along the increase of the segments. Since the resulting curves have to describe real tooth profiles, there is still a number of restrictions that exclude a number of them. Therefore, all the control points that lay under the line that connects P_0 and P_3 are excluded, along with those that result in a slope larger than 70^0 at the beginning of the curve (this late value was found to be a threshold above which the resulting profile does not follow the law of gearing). Non-acceptable profiles result also if P_1 lays on the left of P_2 on the above graph. Following these remarks, from the equations 23 to 24 we obtain the Bezier curve for BC tooth segment and implementing the law of gearing we obtain its corresponding symmetrical AB segment. Fig. 3 gives a result for number of teeth equal to 6 and slope value on B point equal to 51.41^0, generated by Bezier polynomials. It is important to note that all of the following figures would depict half of the corresponding teeth profiles (π/z).

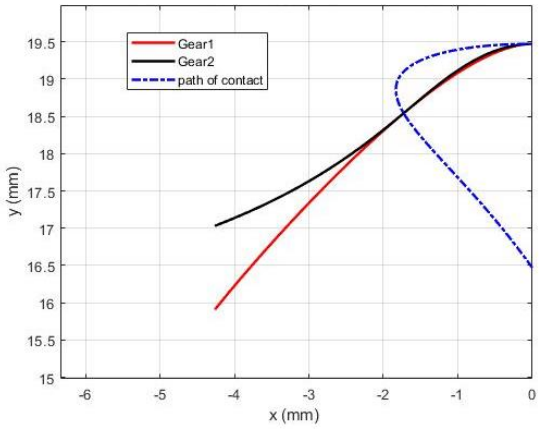

Fig. 3. Bezier teeth pair: z=6, slope 51.41^0 .

4 Optimization threshold in symmetrical tooth profiles

There are several geometrical elements that restrict further optimization of the derived profiles. These are: the tooth tip radius R_k and the center distance α_{12} which defines the radius on the pitch circle. Having these two values fixes, the tooth height α, could be further deducted and it has the same value for all the separate profiles that are generated. Furthermore, as it has already

been stated, for the symmetrical profiles, the tooth depth β is also defined and equals α. Therefore, the optimum delivery fluctuation that could be obtained from the profiles to be studied is predefined as long as these parameters are selected.

Three types of closed path of contact symmetrical profiles are going to be studied, the sinusoidal, the polynomial and the Bezier profiles. For the sinusoidal, for every tooth number, just one profile is derived. However, for the polynomial and Bezier curve profiles, there is a group of possible curves associated with every teeth number. The elements of each of these group have a predefined flow delivery fluctuation, however, each different form is associated with a different derivative of this fluctuation profile. The importance of this derivative and its association with the secondary delivery fluctuation due to a non-constant pressurization of pump's chambers, would be following denoted as "acceleration term'.

Another important observation that came out from the simulations is that for every symmetrical close path of contact gear pump, there is a circle of radius a, the center of which lays on the contact point on the pitch circle, that acts as a threshold for optimisation on the fluctuation ripple. Therefore, in order for a contact pair to have an optimum value for the flow ripple, it should be associated with a path of contact that lays beneath that circle. A graphical explanation of this remark is depicted in the following figure.

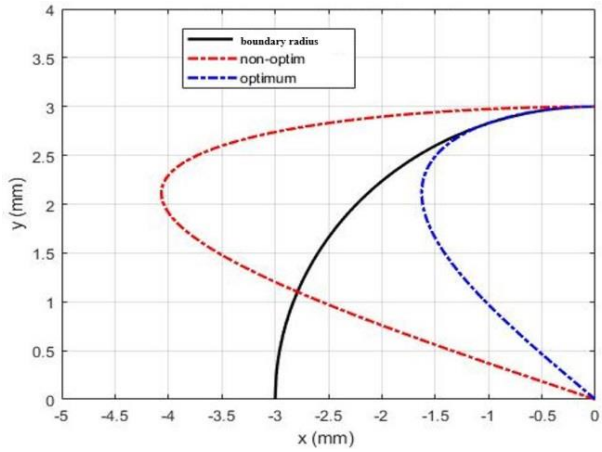

Fig. 4. Path of contact boundary shape.

5 Flow ripple characteristics in various designs

5.1 Sinusoidal teeth

As it was stated, the predefined form of sinusoidal equations, do not provide the ability of profile parametrization for a given teeth number. However, since the form of these curves obeys the rules described for the symmetrical closed path of contact gears, its optimum values are given for low teeth number and in particular for teeth number up to 5. It is evident that it could not be done any further selection in respect to the acceleration term, since its derivative is also predefined for a given teeth number. The following figure depicts the optimum profile made from a sinusoidal rack along with the associated flow ripple and its acceleration parameter.

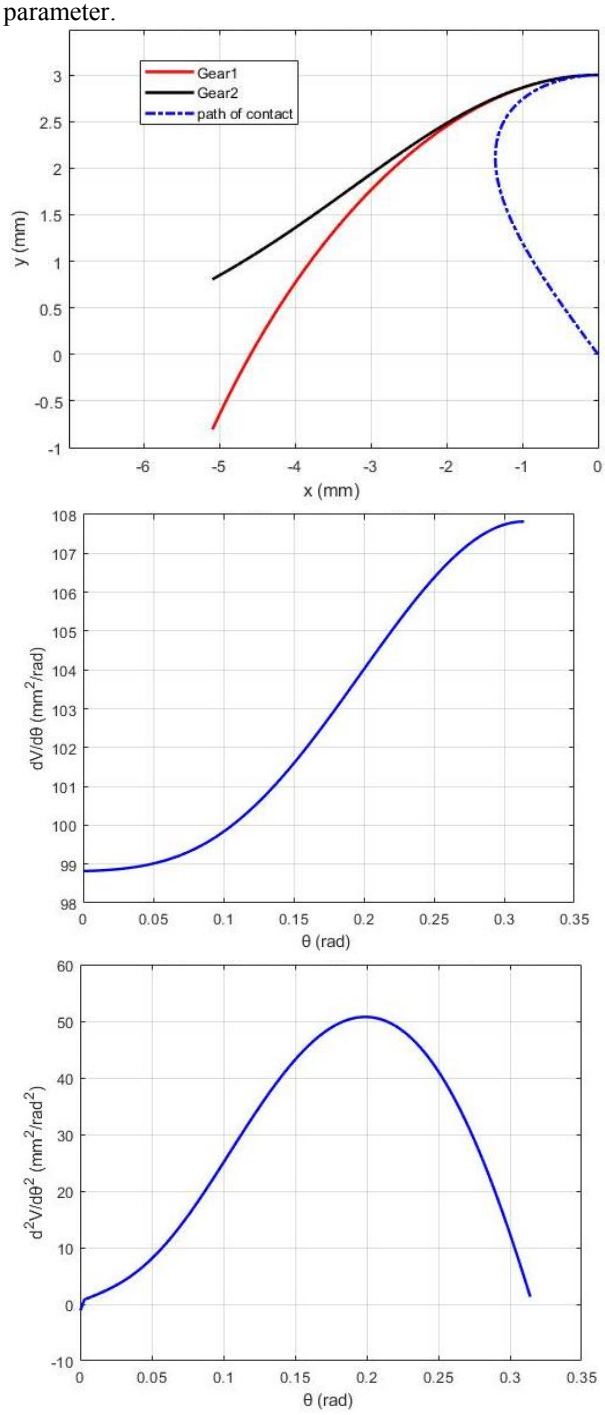

Fig. 5. Optimum sinusoidal teeth for z=5.

The flow ripple for this curve was 4.36%. It can easily be observed that the flow elements are smoothly altered with respect to the angular rotation. This occurs due to the nature of the curve, but also due to the low teeth number.

5.2 Polynomial Teeth

In this case the derived profiles are generated through cubic polynomial curves as described in [10]. Changing the parameter a_3 of the polynomial equation provides the

ability of designing a whole set of these curves. However, it is not possible to produce optimum curves for every teeth number, since there is a critical point where the generated path of contact surpasses the circle that defines the optimum envelope, as described above. Simulations proven that the maximum teeth number up to which we could obtain optimum curves was equal to 6. Therefore, for this teeth number, a group of profiles was generated by altering the value of a_3. As described, the delivery fluctuation was the same for every element of the group. The selection for group's optimum was made based on the acceleration term that defines the developed pump pressure. Following figure depicts the selected polynomial curve for flow ripple equal to 4.36% and teeth number equal to 6.

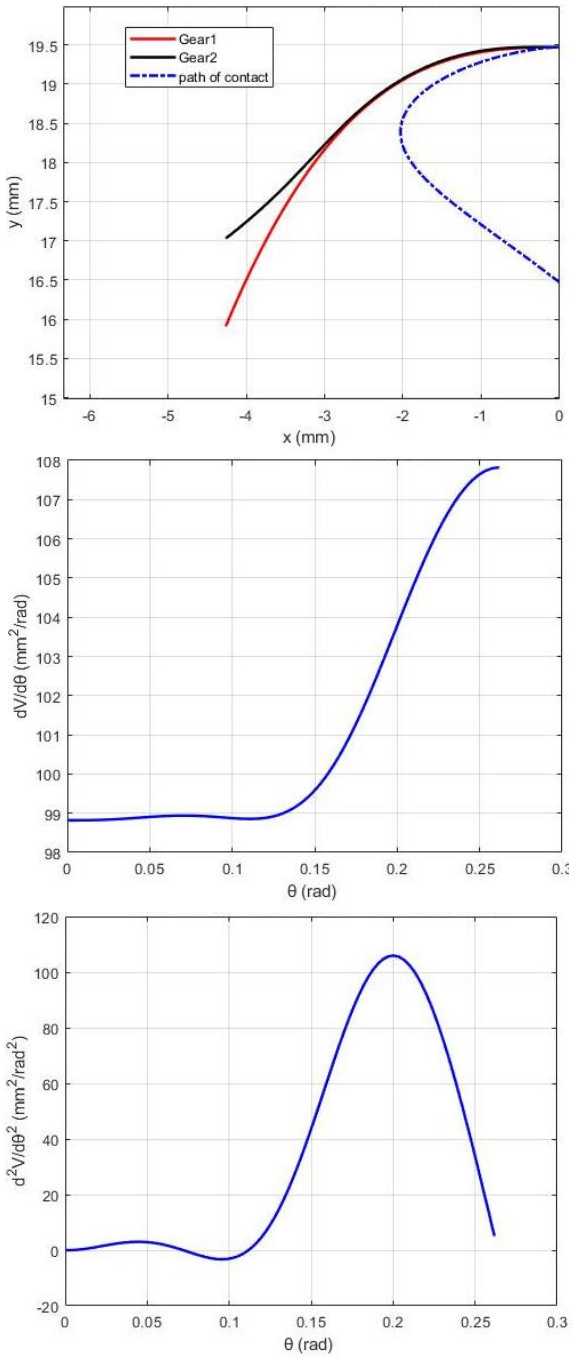

Fig. 6. Optimum polynomial teeth for z =6.

5.3 Bezier teeth

In the Bezier curves case, there is also a group of tooth profiles that for a given teeth number have an optimum value for the flow delivery fluctuation. However, the flexibility provided by control points that generate the curve, gives possibility to explore a wider range of curves on their acceleration term. Furthermore, this flexibility also affects the maximum number of teeth based on which the optimum curves can be generated. The following figure depict the selected curve which provides optimum flow ripple of 4,46% and also carry the optimum performance on the acceleration parameter and its number of teeth equal to 8.

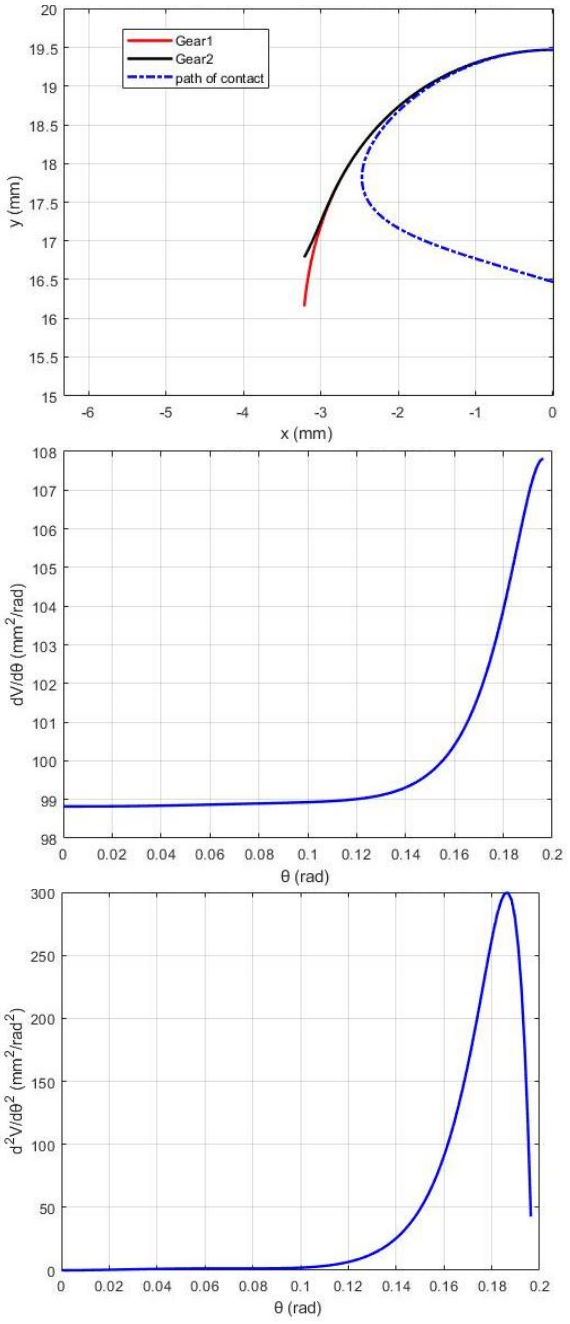

Fig. 7. Optimum Bezier teeth for z =8.

6 Benchmark

Following table presents the results for the flow elements that were derived from these profile types and the equivalent (in terms of absolute flow delivery involute gear pump).
It can be therefore easily seen that the optimisation of the symmetrical closed path of contact gear pump could lead to flow ripple reduction over standard involute gear pump. Their significant advantage is also evident in the acceleration term as well. It is also important to note the observation that teeth number increase leads to a slight decrease of the flow delivery, contrary to the involute pumps, something that offers a further design flexibility. Therefore, future steps of research is manufacturing of the presented gears, in order to verify experimentally the presented work and also to further investigate vibration and noise that they induce to the upstream hydraulic system.

Table 1. Results for sinusoidal teeth.

Teeth	Flow ripple (%)	Flow Per rad mm^2	Acc. term Mean Value $\frac{mm^2}{rad^2}$	Acc. term Deviation $\frac{mm^2}{rad^2}$
2	4.36	324.34	11.30	5.66
3	4.36	323.85	16.86	8.66
4	4.36	323.15	22.24	12.33
5	4.36	322.24	27.25	17.48

Table 2. Results for polynomial teeth.

Teeth	Flow ripple (%)	Flow Per rad mm^2	Acc. term Mean Value $\frac{mm^2}{rad^2}$	Acc. term Deviation $\frac{mm^2}{rad^2}$
2	4.36	324.07	11.27	7.77
3	4.36	322.19	16.19	11.65
4	4.36	320.93	20.95	17.06
5	4.36	319.58	25.26	25.35
6	4.36	317.98	28.94	38.40

Table 3. Results for Bezier teeth.

Teeth	Flow ripple (%)	Flow Per rad mm^2	Acc. term Mean Value $\frac{mm^2}{rad^2}$	Acc. term Deviation $\frac{mm^2}{rad^2}$
2	4.36	327.65	9.73	7.52
3	4.36	326.46	14.63	10.32
4	4.36	322.18	19.80	12.35
5	4.36	322.39	22.35	18.34
6	4.36	319.55	26.82	26.45
7	4.36	317.65	32.66	41.83
8	4.36	313.97	56.43	92.03

Table 4. Results for involute teeth**.**

Teeth	Flow ripple (%)	Flow Per rad mm^2	Acc. term Mean Value $\frac{mm^2}{rad^2}$	Acc. term Deviation $\frac{mm^2}{rad^2}$
10	10.94	317.76	8.6169	118.255

It can be therefore easily seen that the optimisation of the symmetrical closed path of contact gear pump could lead to flow ripple reduction over standard involute gear pump. Their significant advantage is also evident in the acceleration term as well. It is also important to note the observation that teeth number increase leads to a slight decrease of the flow delivery, contrary to the involute pumps, something that offers a further design flexibility. Therefore, future steps of research is manufacturing of the presented gears, in order to verify experimentally the presented work and also to further investigate vibration and noise that they induce to the upstream hydraulic system.

References

1. T.Costopoulos, A.Kanarachos, E.Pantazis (1987): Reduction of delivery fluctuation and tooth profile of spur gear rotary pumps, Mechanisms and Machine Theory, vol**.** **23**, pp. 141-146.
2. Bosch Rexroth AG, SILENCE PLUS: The next generation of external gear pumps.
3. N.Maring, S.Kasaragadda, (2003): The theoretical flow riplle of an external gear pump, Transactions of the ASME, vol. **125**, pp. 396-404.
4. A.Vacca, M.Guidetti (2011): Modelling and experimental validation of external spur gear machines for fluid power applications, Simulation Modelling Practice and Theory, vol. **19**, pp. 2007-2031.
5. K.Huang, W.Lian (2009): Kinematic flowrate characteristcs of external spur gear pumps using an exact closed solution, Mechanisms and Machine Theory, vol. **44**, pp. 1121-1131.
6. K. Nagamura, K.Ikejo, F.G. Tutulan (2004): Design and performance of gear pumps with non-involute tooth-profile, Proceedings of the Institution of Mechanical Engineers Part B: Journal of Engineering Manifacture, vol. **218**, pp. 699-710.
7. Y.W. Liu, K.Tang (2004): The design of assymetric spur gear pump with crisscross spur structures, Journal of Dalian Railway Institute, vol. **25**, pp. 28-30.
8. V.Spitas, T. Costopoulos, C.Spitas (2007): Fast modelling of conjugate gear tooth profiles using discrete presentation by involute segments, Mechanisms and Machine Theory, vol. **42**, pp. 751-762
9. Prautzsch, H., Boehm, W., & Paluszny, M. (2013).*Bézier and B-spline techniques*. Springer Science & Business Media.
10. Tsolakis, E., & Spitas, V. Optimised Tooth Flank Geometry For Minimizing Delivery Fluctuation In Hydraulic Gear Pumps With External Teeth, Proc. of the International Conference on Power Transmission "BAPT 2016.